QUANTITATIVE CHARACTERIZATION OF THE LATERAL DISTRIBUTION OF MEMBRANE PROTEINS WITHIN THE LIPID BILAYER

ERNESTO FREIRE AND BRIAN SNYDER
Department of Biochemistry, University of Virginia School of Medicine, Charlottesville, Virginia 22908

ABSTRACT The dependence of the lateral distribution of membrane proteins on the protein size, protein/lipid molar ratio, and the magnitude of the interaction potentials has been investigated by computer modeling protein-lipid distributions with Monte Carlo calculations. These results have allowed us to develop a quantitative characterization of the distribution of membrane proteins and to correlate these distributions with experimental observables. The topological arrangement of protein domains, protein plus annular lipid domains, and free lipid domains is described in terms of radial distribution, pair connectedness, and cluster distribution functions. The radial distribution functions are used to measure the distribution of intermolecular distances between protein molecules, whereas the pair connectedness functions are used to estimate the physical extension of compositional domains. It is shown that, at characteristic protein/lipid molar ratios, previously isolated domains become connected, forming domain networks that extend over the entire membrane surface. These changes in the lateral connectivity of compositional domains are paralleled by changes in the calculated lateral diffusion coefficients and might have important implications for the regulation of diffusion controlled processes within the membrane.

INTRODUCTION

During the past few years it has become evident that the molecular constituents of biological membranes are not distributed at random within the bilayer matrix and that their distribution can be altered by external physicochemical variables or during the course of specific biological processes (1–4). Studies on model membranes and reconstituted systems have demonstrated that many physical and functional properties of the membrane are sensitive to the particular way in which lipid and protein molecules are distributed within the bilayer (5–7). Recently, it has been shown that diffusional processes within the plane of the membrane are strongly affected by the topological arrangement of membrane components, particularly by the existence of a highly connected network of fast diffusion compositional domains (8–10).

Since biological membranes are heterogeneous systems characterized by the presence of physically distinct and topologically irregular lipid and protein domains, it is not generally possible to develop complete analytical descriptions of the planar distribution of lipid and protein molecules. An alternative approach to the study of membrane organization involves the use of computer-generated molecular distributions. Previously, we developed a system of Monte Carlo calculations directed to generate lipid distributions with the computer (11, 12). This method has been applied to the study of the lateral distribution of molecules in binary mixtures of phosphatidylcholines, cholesterol-phosphatidylcholines, and cholesterol-sphingomyelin mixtures (9, 11, 12). In this paper we present a generalization of this method to include molecules of different cross sectional areas and various interaction potentials. Particularly, we have been interested in computer modeling the planar distribution of membrane proteins and its dependence on protein size, protein/lipid ratio, and interaction energies. We also attempt to identify the organizational parameters that are relevant to specific membrane properties and to provide a rigorous way of characterizing the lateral distribution of membrane proteins. Analysis of the experimentally derived organization parameters as described in the text should provide information regarding the exact nature of protein-protein and protein-lipid interactions. Preliminary results of this work were presented at a meeting of the Biophysical Society (13).

THEORY

There are two distinct aspects to the problem of modeling molecular distributions for membrane systems by computer. The first concerns the development of a representation formalism capable of providing an accurate and quantitative picture of the membrane, and the second is associated with the development of the generating algo-

Dr. Freire's present address is Department of Biochemistry, University of Tennessee, Knoxville, TN 37916

rithm or algorithms directed to produce the desired molecular distributions. In the first paper of this series (11) we developed a matrix formalism to represent the lateral distribution of molecules in binary mixtures of lipids. This matrix formalism has now been generalized to include molecules of different cross sectional areas such as in the case of biological membranes containing different types of protein and lipid molecules.

For a given composition, the distribution of molecules within the lateral plane of the membrane is dictated by the magnitude of the interaction potentials between the various membrane components. The magnitude of these interactions can be affected by external physicochemical parameters (temperature, ligand molecules, pH, Ca^{2+} concentration, etc.) that can trigger lateral reorganization processes within the membrane. To represent these phenomena we have developed a generating algorithm that reflects the molecular interactions, thus providing a way to establish quantitative correlations between energetic and organizational parameters.

Representation Matrix

The membrane surface is represented by an $m \times n$ matrix $D = \| D_{ij} \|$ (see Appendix) in which the matrix elements D_{ij} represent surface elements with position coordinates centered at i, j. For mathematical convenience these surface elements are assumed to be hexagonally packed, forming a triangular lattice. This assumption does not impose any restriction upon the membrane system, since it is only related to the internal structure of the representation matrix. Each matrix elements D_{ij} can be further specified ($D_{ij} \rightarrow D_{ij,k}$) so that it contains information regarding any desired property, k, of the membrane at (i, j). An illustrative example of this type of matrix representation is shown in Fig. 1.

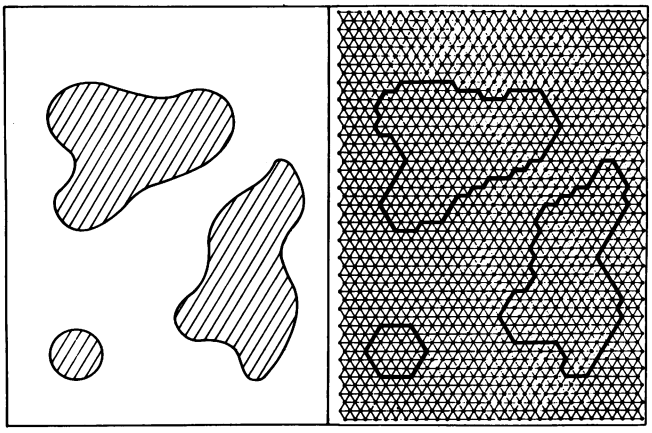

FIGURE 1 Representation of continuous geometrical shapes (left panel) using a triangular lattice (right panel). The resolution with which an image is represented is dictated by the lattice spacing d_0. A scaling transformation is used to increase or decrease the resolution (see Appendix).

The resolution with which the membrane surface is represented is dictated by the resolution length, d_0. The resolution can be increased or decreased by scaling the resolution length. As demonstrated in the Appendix this scaling process changes the size of the D matrix but does not affect the triangular structure of the lattice. For actual computations, limited by the storage capacity of the computer, a compromise should be made between the total surface area to be represented and the desired resolution, since the matrix size grows as d_0^{-2}. In this paper, we shall use the mean separation distance between lipid molecules as a unit of length. This is equivalent to a resolution of 8–10 Å.

Membrane Proteins

A protein molecule embedded within the bilayer lattice can be represented as an amorphous cylinder of height H_P and mean molecular radius R_P. In terms of the representation matrix D, the cross-sectional area occupied per protein molecule can be expressed in terms of the number of surface elements D_{ij} required to cover an area similar to that of one protein molecule. Owing to the triangular structure of the representation matrix, it is possible to express all the parameters necessary to specify a protein molecule in a very simple and compact form. If (i_0, j_0) represent the coordinates of the center of mass of a protein molecule, it is possible to draw concentric hexagons centered at (i_0, j_0) and separated by d_0, so that the nth hexagon contains the position coordinates of exactly $6n$ surface elements D_{ij}. If B denotes the maximum number of concentric hexagons that can be inscribed within the area occupied per protein molecule, it can be shown that

$$B = \mathrm{INT}\left(\frac{R_P}{d_0} - \frac{1}{2}\right) + \mathrm{INT}\left[2\,\mathrm{FRC}\left(\frac{R_P}{d_0} - \frac{1}{2}\right)\right], \qquad (1)$$

where INT and FRC denote the integer and fractional part of a function, respectively. The protein molecule occupies a surface area similar to that occupied by σ surface elements D_{ij}, where

$$\sigma = 1 + 3B(B + 1). \qquad (2)$$

The central coordinates of the potential nearest neighbor protein molecules of any given protein lie on the hexagon at

$$H = 2B + 1. \qquad (3)$$

The region between H and B is the excluded area region and cannot contain the central coordinates of another protein. For each protein molecule there are $6H$ potential nearest neighbor positions of which at most six can be occupied.

The number of lipid molecules surrounding a protein molecule (annular lipid) is given by

$$n_{L,A} = \gamma\, 6\,(B + 1), \qquad (4)$$

where $\gamma = 2$ for a transmembrane protein and $\gamma = 1$ for a protein that spans half of the bilayer.

Lateral Distribution of Protein Molecules

The lateral distribution of protein centers of mass is determined by an effective interaction potential between protein molecules. This interaction potential consists of two parts: (*a*) A hard core potential, which limits the closest approach of two centers of mass to $2R_P$; and (*b*) an attractive/repulsive radial potential which reflects the energetics of the interaction between two protein molecules. In this paper we shall assume that this radial potential extends only to nearest neighbor protein molecules; the generalization to other interaction potentials is straightforward. Moreover, the existence of an impenetrable layer of annular lipid can be easily incorporated into the formalism by increasing the distance of closest approach between protein molecules. Even though the above assumptions might not be entirely realistic, especially for those cases in which the distribution of protein molecules is constrained by a cytoskeleton, they nevertheless constitute a starting point from which more complex interactions can be identified and evaluated. As noted previously, the representation model is phenomenologically oriented so that different interaction potentials can be incorporated and the resulting distributions compared with those observed experimentally. Under the present assumptions, the magnitude of the interaction determines the state of aggregation of the protein molecules and can be expressed in terms of a single Boltzmann exponent $P\alpha \exp[-E(R)/kT]$ (11). The parameter P has the meaning of an affinity constant, so that a $P > 1$ reflects an attractive potential between protein molecules, a $P < 1$ reflects repulsive interaction between protein molecules, and a $P = 1$ characterizes the situation in which the only interactions are excluded volume interactions dictated by the hard core potential.

The generation of protein-lipid distributions with the computer is achieved by successive incorporation of protein molecules into an initially pure lipid lattice (for details see 9, 11, 12). The probability for protein insertion at any given site (i, j) is expressed in terms of the Boltzmann exponent P. The intrinsic statistical weight, $W_{i,j}$, for protein insertion at i, j, is calculated as follows: $W_{i,j} = 0$ if the site is already occupied or lies within the excluded area region of another protein molecule; or $W_{i,j} = p^k$ if the site is on the nearest neighbor hexagon of k other protein molecules. In this way, protein-lipid distributions as a function of the protein/lipid ratio, protein size, and interaction potential can be obtained. The resulting output of each computer experiment is an $m \times n$ matrix in which the lattice positions occupied by protein molecules, annular lipid, and bulk lipid are denoted by a different integer. Each matrix is then directly analyzed with the computer to obtain the desired lateral organization parameters. Of particular importance for a quantitative characterization of protein-lipid systems are (*a*) the radial distribution function for protein molecules, (*b*) the state of aggregation of protein molecules, and (*c*) the physical extension of protein domains, protein plus annular lipid domains, and free lipid domains. All organizational parameters are calculated according to the methods described previously (11, 12). It is important to note that these organizational parameters can be obtained experimentally, thus providing a way to establish precise correlations between molecular interactions and lateral organization.

RESULTS

Radial Distribution Function

The radial distribution function $g_{BB}(d)$ measures the distribution of intermolecular distances for molecules of type B within the lateral plane of the membrane. It is defined as the ratio between the molecular density $X_B(d)$ and the average density X_B. $g_{BB}(d)$ is zero for distances smaller than the exclusion radius and usually has a well defined peak at the distance of closest approach between molecules. As the separation distance, d, increases $g_{BB}(d)$ approaches a final value of unity. The existence of peaks at intermediate separation indicates preferred interaction distances. The amplitude of these peaks is a function of the molecular density and the magnitude of the interaction potentials.

The above concepts are illustrated in Fig. 2 for the case of a protein molecule with a cross sectoinal area nine times larger than that of a lipid molecule ($R_P/R_L = 3$). The distributions in this figure were generated with only the hard core potential as a constraint (i.e., $P = 1$). As shown in the figure, $g_{BB}(d)$ is zero for distances smaller than the excluded radius and has a pronouced maximum at the

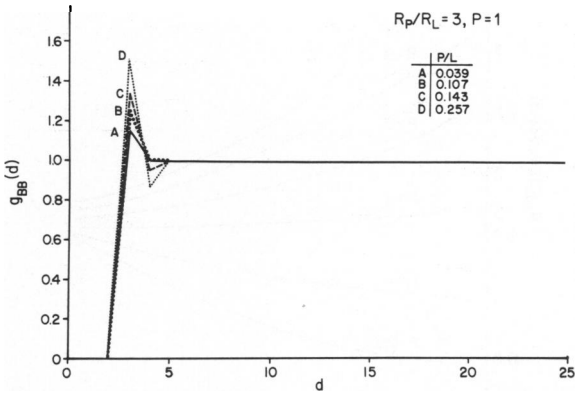

FIGURE 2 Dependence of radial distribution function, $g_{BB}(d)$ on protein/lipid ratio for $R_P/R_L = 3$ and $P = 1$. As described in the text, the unit of length was chosen to be the mean separation distance between lipid molecules. For these and all calculations throughout this paper the protein/lipid values correspond to proteins that span half of the bilayer. For transmembrane proteins the protein/lipid values should be divided by two.

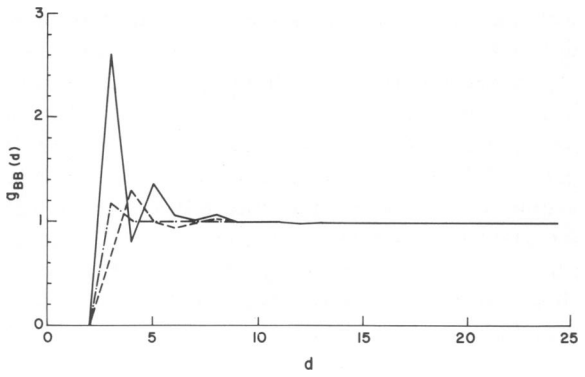

FIGURE 3 Dependence of radial distribution function $g_{BB}(d)$ on the intermolecular potential for $R_P/R_L = 3$ and constant protein/lipid = 0.06. $P = 5$ (—), $P = 1$ (—·—) and $P = 0.2$ (——).

distance of closest approach. The amplitude of this maximum increases as the protein/lipid ratio increases. At large separation, $g_{BB}(d) = 1$, which indicates that the molecular positions become uncorrelated. Fig. 3 shows the effects of an attractive ($P > 1$) and repulsive ($P < 1$) interaction potential on the radial distribution function. An attractive potential induces a large increase in the amplitude of the peak at the distance of closest approach, and gives rise to smaller peaks whose amplitude decreases monotonically as the separation distance increases. A repulsive potential reduces the amplitude of $g_{BB}(d)$ at the distance of closest approach and shifts the position of the maximum to larger separation distances.

In Fig. 4 the magnitude of $g_{BB}(d)$ at the distance of closest approach [$g_{BB}(d$ = closest)] has been plotted as a function of F_A (PROT), the fraction of membrane surface area occupied by protein molecules, for several values of the affinity constant P. This dependence can be used to determine P if the radial distribution function is known. For example, Pearson et al. (14) have been able to estimate from freeze fracture studies the radial distribution function for intramembranous particles in human erythrocyte membranes under several conditions. They found peak amplitudes of 1.25, 1.50, and 1.75 for their experimental groups I, II, and III, respectively. According to these authors the group I membrane is almost intact, group II lacks 70% of its spectrin, and group III has all of its spectrin removed, showing significant amounts of particle aggregation. The particle density in their samples was $\simeq$4,000/μm^2, which corresponds to a F_A (PROT) value of $\simeq$0.3. From our computer-generated distributions we estimate P values of 1.2, 1.8, and 2.4 for experimental groups I, II, and III, respectively. These calculated values are in agreement with the authors' interpretation (14), which also found some nonrandomness in group I and increasing degrees of aggregation for groups II and III. Our calculated P values correspond to effective interaction energies of 110, 350, and 520 cal/mol of intramembranous particles at 25°C.

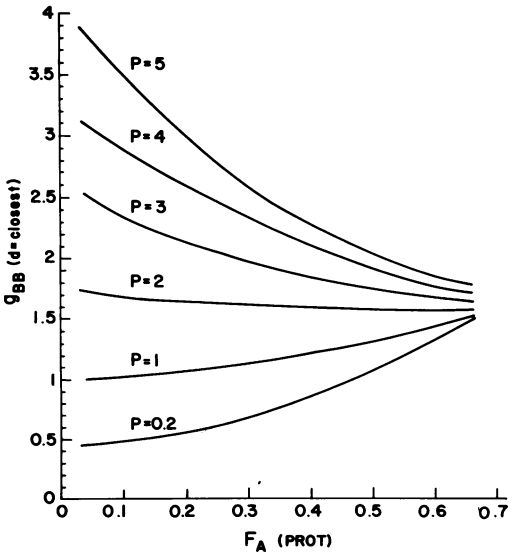

FIGURE 4 Dependence of the amplitude of the peak in the radial distribution fraction, g_{BB} (d = closest), on F_A(PROT), the fraction of membrane surface area occupied by protein molecules for several values of the affinity constant P.

State of Aggregation and Lateral Connectivity of Protein Domains

The state of aggregation of protein molecules can be quantitatively studied by introducing a cluster distribution function that counts the number of protein molecules populating clusters of size n. Typical examples of cluster distribution functions are given in Fig. 5 for $R_P/R_L = 3$, $P = 1$, and $R_P/R_L = 3$, $P = 3$. In this figure, the fraction of protein molecules in clusters of size n has been plotted as

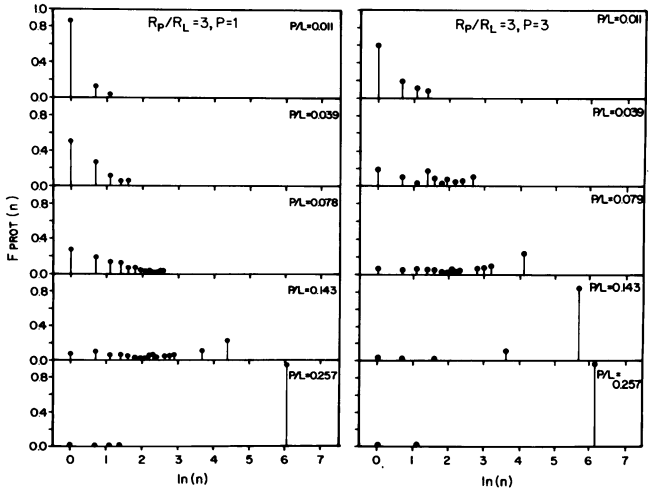

FIGURE 5 Typical cluster distribution functions for membrane proteins. Shown are the fractions of protein molecules in clusters of size n as a function of ln(n) for several protein/lipid molar ratios and two different values of the affinity constant P.

a function of the natural logarithm of the cluster size for several protein/lipid ratios. For any given protein concentration the distribution is shifted to larger cluster sizes as the protein-protein affinity constant P increases. These distributions allow calculation of the mean size of protein aggregates and its dependence on the protein/lipid ratio and the interaction energies between protein molecules.

A characteristic feature of these cluster distributions is the existence of an abrupt change in their character at some critical protein/lipid ratio. Below the critical concentration the system is characterized by the presence of isolated clusters, whereas above the critical concentration the clusters become connected, forming a single network that contains most of the protein molecules. This phenomenon, technically called percolation, has been previously described for lipid mixtures (12) and cholesterol-lipid mixtues (9), and has been shown to have important effects on lateral diffusion processes.

In the case of protein-lipid systems it is possible to define three different states of aggregation in relation to the lateral connectivity of the free lipid, annular lipid, and protein domains. These possible states of aggregation are illustrated in Fig. 6. In this figure, panel A represents a situation in which the protein molecules plus their annular lipid (stippled areas) are dispersed and isolated within the bilayer. Panel B represents a situation in which the annular lipid has become connected and the protein molecules "float" in a continum of annular lipid; this situation is also characterized by the disruption of the free lipid into isolated compartments. Finally, panel C represents a situation characterized by massive protein-protein contacts leading to the disruption of the annular lipid as well as the free lipid.

The above distributions can be quantitatively characterized in terms of the pair connectedness function $C_{BB}(d)$. $C_{BB}(d)$ is equal to the probability that two molecules of type B separated by a distance d belong to the same cluster (9, 12). The probability that the physical extension of a given compositional domain is of the order of the membrane dimensions is given by $C_{BB}(d_{max})$, where d_{max} is

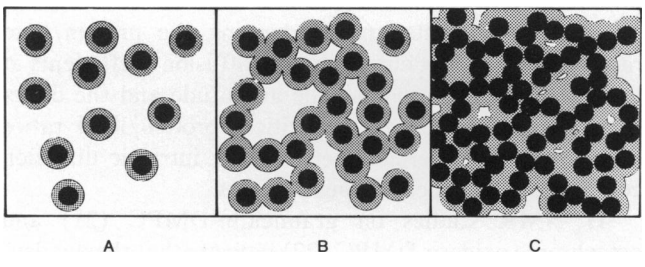

FIGURE 6 Three different cases of protein aggregation. (A) Protein molecules (black circles) plus annular lipid (stippled areas) are isolated and dispersed throughout the membrane surface. (B) The annular lipid is connected forming a continuum throughout the membrane; note that the free lipid (white areas) has been disrupted into isolated compartments. (C) Very high protein density leading to the disruption of annular and free lipid.

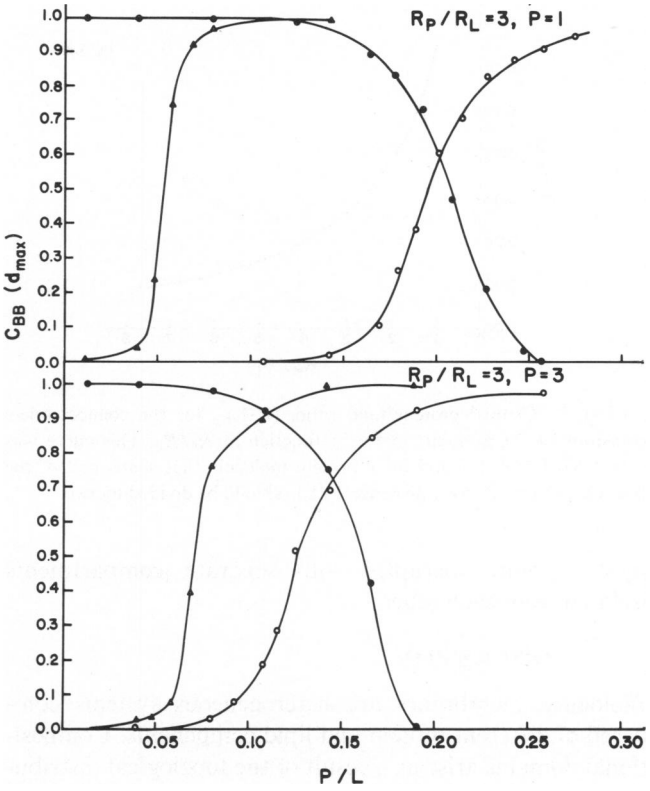

FIGURE 7 Pair connectedness function at maximum separation within the membrane, $C_{BB}(d_{max})$, as a function of the protein/lipid ratio for P = 1 and P = 3. Annular lipid (△); annular plus free lipid (●), and protein molecules (○).

the maximum separation distance within the bilayer. Below the percolation threshold $C_{BB}(d_{max})$ is negligible, whereas above the percolation threshold $C_{BB}(d_{max})$ approaches the value of unity, which indicates that previously isolated clusters have become connected, forming a network that extends over the entire bilayer surface.

In Fig. 7, $C_{BB}(d_{max})$ has been plotted as a function of the protein/lipid molar ratio for the free lipid, annular lipid, and protein molecules. As shown in the figure, the various domains undergo a dramatic change in their lateral connectivity at characteristic protein/lipid ratios. A salient feature of these connectedness transitions is that in all cases they occur over narrow concentration intervals. The critical protein/lipid ratios are functions of R_P/R_L, the ratio between the protein and lipid molecular radius, and P, the affinity constant between protein molecules. As shown in the figure, the critical concentration for the protein transition is strongly dependent on P, whereas the critical concentration for the annular lipid is somewhat less sensitive to the actual value of P. The dependence of the critical protein/lipid ratio on R_P/R_L for the annular lipid is shown in Fig. 8. In this figure $(P/L)_C$ represents the protein/lipid molar ratio at which the annular lipid become connected and the protein molecules "float" in a continuum of annular lipid. At this concentration the free

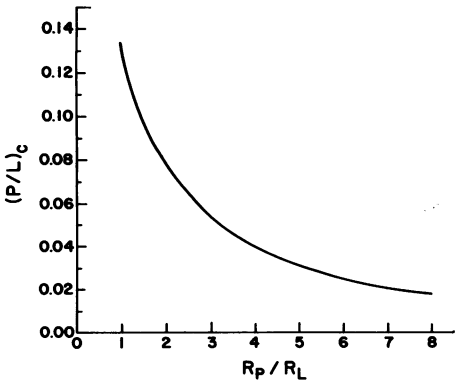

FIGURE 8 Critical protein/lipid ratio, $(P/L)_C$, for the connectedness transition of the annular lipid as a function of R_P/R_L. This curve was calculated for $P = 1$ and for a protein molecule that spans half of the bilayer. For transbilayer proteins $(P/L)_C$ should be divided by two.

lipid becomes disrupted into separate compartments isolated from each other.

DISCUSSION

Biological membranes are heterogeneous systems composed of different protein and lipid components. Compositional domains arise as a result of the topological distribution of these components within the bilayer matrix. The actual size, number, and geometry of these domains are determined by the magnitude of the interactions between the various components. Since these interactions can be affected by external physicochemical variables, changes in the chemical or physical environment will often trigger lateral reorganization processes and affect functional properties of the membrane. The existence of compositionally distinct domains may influence functional properties of the membrane either by defining local environments with specific properties or by affecting the large scale organization of the membrane. A complete understanding of these effects requires the development of a quantitative characterization of the lateral distribution of molecules within the bilayer, so that organizational parameters can be correlated with physical properties of the membrane. These studies are designed to develop a unified representation of the lateral organization of biological membranes and to identify the organizational parameters relevant to various biological processes.

Previous theoretical and experimental studies have focused on the molecular aspects of protein-lipid interactions and the local perturbations that protein molecules exert on the surrounding lipid. Our studies have aimed to investigate long-range effects induced by short-range interactions. We have made computer models of protein-lipid systems, assuming that the distribution of protein molecules within the lateral plane of the bilayer is dictated by an effective intermolecular potential expressed as an affinity constant P. This parameter P can be experimentally evaluated from freeze fracture electron micrographs as discussed above, or from the compositional dependence of an appropriate physical observable (Snyder and Freire, paper in preparation).

Even though our calculated protein distributions are independent of the existence of a boundary lipid, we have divided the lipid population into annular and free lipid. The annular lipid has been considered to be a single layer of lipid surrounding the protein molecules. Experimental support for this assumption comes from calorimetric and spectroscopic evidence. Calorimetric scans of protein-lipid systems indicate that the number of lipid molecules participating in the lipid phase transition diminishes upon increasing the protein/lipid ratio. The actual number of lipids subtracted from the transition per protein molecule can be estimated from the initial slope of ΔH vs. protein/lipid plot (15). Analysis of the data for gramicidin (16), melittin (Freire, unpublished results), and Ca^{2+} ATPase from sarcoplasmic reticulum (17) yields values of 6, 16, and 43, respectively for the number of lipid molecules withdrawn from the transition per protein molecule. These numbers are proportional to the molecular dimensions of the protein molecules and equivalent to the number of lipid molecules required to cover the perimeter of one protein. Similar conclusions have been obtained with electron spin resonance (18–20), nuclear magnetic resonance (18, 20), and Raman spectroscopy (16, 20).

The resulting computer generated distributions contain protein domains, protein plus annular lipid domains, and free lipid domains. The distribution of lipid domains and the relative population of annular and free lipid are dictated by the lateral distribution of protein molecules. This distribution is best characterized in terms of the radial distribution function, as was also demonstrated by Pearson et al. (14).

The physical extension of protein, annular, and free lipid domains is measured in terms of pair connectedness functions. These functions are negligibly small at low concentrations but increase abruptly at the critical protein/lipid ratio in which domain percolation occurs. Dynamic Monte Carlo calculations (Van Osdol et al. manuscript in preparation) based upon our calculated protein-lipid distributions predict a decrease in the lateral diffusion coefficients upon increasing the protein/lipid ratios and an abrupt change in the diffusion coefficients at the percolation thresholds. The amplitude and the direction of the changes at the critical protein/lipid ratios depend on the difference between the intrinsic diffusion coefficients of the percolating domains.

^2H NMR studies on gramicidin-DMPC (21) and cytochrome oxidase-DMPC (22) indicate that the quadrupole splittings, $\Delta\nu_Q$, increase at low protein/lipid ratios until they reach a maximum value and then decrease precipitously at higher protein/lipid ratios. This behavior indicates a disordering effect at low protein/lipid ratios and an ordering effect at high protein concentrations (21). It is interesting to note that for both protein systems the

position of the maximum in $\Delta\nu_Q$ coincides with the protein/lipid ratio at which the annular lipid becomes connected and the free lipid is disrupted into isolated compartments. Similar ^2H NMR studies on cholesterol-DMPC (23) have shown that the quadrupole splitting is maximal at 20 mol % cholesterol, i.e., the concentration at which the cholesterol rich domains become connected and the free lipid is disrupted (9). These observations suggest the existence of strong correlations between local order parameters and the long-range organization of the membrane. Future work should elucidate the precise nature and the biological implications of these effects. In this work we have computer modeled protein distributions in terms of an effective radial potential that modulates the state of protein aggregation. In a future paper the effects of specific interactions leading to the formation of well defined structural patterns on the membrane surface will be presented.

APPENDIX

Matrix Representation

A two-dimensional surface of total area S can be mathematically represented by an $m \times n$ matrix $D \parallel D_{ij} \parallel$, in which the matrix elements D_{ij} denote elementary surface elements with position coordinates centered at i, j. The actual value of D_{ij} can be used to describe any property of the surface element centered at i, j. The area, δS, of each surface element D_{ij} is equal to $S/(m \cdot n)$ and defines the "resolution" with which continuous functions can be represented. In principle, δS can be made arbitrarily small by increasing the size of the matrix D, so that any desired degree of resolution can be obtained.

For mathematical convenience we assume that the surface elements D_{ij} are hexagonally packed, forming a triangular lattice. In that case a two-dimensional surface of total area $S \equiv h \times l$ can be represented with a resolution length d_0 with a matrix of order

$$m = \frac{2h}{\sqrt{3}\, d_0}; \qquad n = \frac{l}{d_0}. \tag{A1}$$

Scaling

Changes in resolution can be obtained by scaling the resolution length. An nth order scaling corresponds to a 2^{-n} reduction in the resolution length. After a nth scaling $d_n = d_0 2^{-n}$, and the coordinates of the point (i_0, j_0) become

$$i_n = 2^n(i_0 - 1) + 1, \tag{A2}$$

$$j_n = 2^n(j_0 - 1) + 1. \tag{A3}$$

It must be noted that a triangular lattice is invariant under a nth scaling, i.e., the lattice remains triangular under any scaling transformation. This is not true for a square lattice, for example.

Metric

The distance R between any two points (i, j) and (i', j') is given by

$$R = \sqrt{X^2 + Y^2}, \tag{A4}$$

where

$$Y = |i' - i| \frac{\sqrt{3}}{2} d, \tag{A5}$$

$$X = \left[|j' - j| + \tfrac{1}{2}\,\mathrm{Sgn}\,(j' - j)\, \epsilon_{i',i} \right] d, \tag{A6}$$

where $\epsilon_{i',i}$ is a parity symbol defined as

$$\epsilon_{i',i} = \begin{cases} 0;\ P_i = P_{i'} \\ +1;\ i' = \text{even},\ i = \text{odd} \\ -1;\ i' = \text{odd},\ i = \text{even}. \end{cases}$$

$\mathrm{Sgn}\,(j' - j) = +1$ if $j' \geq j$, $\mathrm{Sgn}\,(j' - j) = -1$ if $j' < j$.

This work was supported by grants GM-27244 and GM-26894 from the National Institutes of Health.

Received for publication 10 July 1981 and in revised form 22 September 1981.

REFERENCES

1. Shimshick, E. J., and H. M. McConnell. 1973. Lateral phase separation in phospholipid membranes. *Biochemistry.* 12:2351–2360.
2. Hui, S. W., and D. F. Parsons. 1975. Direct observation of domains in wet lipid bilayers. *Science (Wash. D.C.).* 190:383–384.
3. Wallace, B., and D. Engelman. 1978. The planar distribution of surface proteins and intramembrane particles in *Acholeplasma* laidlawii are differentially affected by the physical state of membrane lipids. *Biochim. Biophys. Acta.* 508:431–449.
4. Van Dijck, P. W. M., B. de Kruijff, A. J. Verkleij, L. L. M. Van Deenen, and J. de Gier. 1978. Comparative studies on the effects of pH and Ca^{2+} on bilayers of variously negatively charged phospholipids and their mixtures with phosphatidylcholine. *Biochim. Biophys. Acta.* 512:84–96.
5. Taylor, R. B., W. P. H. Duffus, M. D. Ruff, and S. De Petris. 1971. Redistribution and pinocytosis of lymphocyte surface immunoglobulin molecules induced by anti-immunoglobulin antibody. *Nature (Lond.).* 233:225–230.
6. Papahadjopoulos, D., W. J. Vail, N. A. Pangborn, and G. Poste. 1976. Studies on membrane fusion. II. Induction of fusion in pure phospholipid membranes by calcium ions and other divalent metals. *Biochim. Biophys. Acta.* 448:265–283.
7. Satir, B. 1976. Genetic control of membrane mosaicism. *J. Supramol. Struct.* 5:381–389.
8. Owicki, J. C., and H. M. McConnell. 1980. Lateral diffusion in inhomogeneous membranes. Model membranes containing cholesterol. *Biophys. J.* 30:383–397.
9. Snyder, B., and E. Freire. 1980. Compositional domain structure in phosphatidylcholine-cholesterol and spingomyelin-cholesterol bilayers. *Proc. Natl. Acad. Sci. U.S.A.* 77:4055–4059.
10. Snyder, B., W. van Osdol, and E. Freire. 1981. Lateral diffusion in multicomponent membranes. *Biophys. J.* 33:163*a*.
11. Freire, E., and B. Snyder. 1980. Estimation of the lateral distribution of molecules in two-component lipid bilayers. *Biochemistry.* 19:88–94.
12. Freire, E., and B. Snyder. 1980. Monte Carlo studies of the lateral organization of molecules in two-component lipid bilayers. *Biochim. Biophys. Acta.* 600:643–654.
13. Freire, E., and B. Snyder. 1981. Development of a general representation of the lateral organization of lipid membranes. Application to protein-lipid systems. *Biophys. J.* 33:161*a*.
14. Pearson, R. P., S. W. Hui, and T. P. Stewart. 1979. Correlative statistical analysis and computer modeling of intramembraneous particle distributions in human erythrocyte membranes. *Biochim. Biophys. Acta.* 557:265–282.
15. Correa-Freire, M. C., E. Freire, Y. Barenholz, R. L. Biltonen, and

T. E. Thompson. 1979. Thermotropic behavior of monoglucocerebroside dipalmitoyl phosphatidylcholine multilamellar liposomes. *Biochemistry.* 18:442–445.

16. Chapman, D., B. A. Cornell, A. W. Eliasz, and A. Perry. 1977. Interactions of helical polypeptide segments which span the hydrocarbon region of lipid bilayers. Studies of the gramicidin A lipid-water system. *J. Mol. Biol.* 113:517–538.
17. Gomez-Fernandez, J. C., F. M. Goni, D. Bach, C. J. Restall, and D. Chapman. 1980. Protein lipid interaction. Biophysical studies of $(Ca^{2+} + Mg^{2+})$-ATPase reconstituted systems. *Biochim. Biophys. Acta.* 598:502–516.
18. Jost, P. C., O. H. Griffith, R. A. Capaldi, and G. Vanderkooi. 1973. Evidence for boundary lipid in membranes. *Proc. Natl. Acad. Sci. U.S.A.* 70:480–484.
19. Marsh, D., A. Watts, W. Maschke, and P. F. Knowles. 1978. Protein-immobilized lipid in dimyristoyl phosphatidylcholine-substituted cytochrome oxidase: evidence for both boundary and trapped bilayer lipid. *Biochem. Biophys. Res. Commun.* 81:397–402.
20. Paddy, M. R., F. W. Dahlquist, J. H. Davis, and M. Bloom. 1981. Dynamical and temperature-dependent effects of lipid-protein interactions. Application of deuterium nuclear magnetic resonance and electron paramagnetic resonance spectroscopy to the same reconstitutions of cytochrome C oxidase. *Biochemistry.* 20:3152–3162.
21. Rice, D., and E. Oldfield. 1979. Deuterium nuclear magnetic resonance studies of the interaction between dimyristoyl phosphatidylcholine and gramicidin A. *Biochemistry.* 18:3272–3279.
22. Kang, S. Y., H. S. Gutowsky, S. C. Hsung, R. Jacobs, R. King, T. E. Rice, D. Chapman, and E. Oldfield. 1979. Nuclear magnetic resonance investigation of the cytochrome C oxidase-phospholipid interaction: a new model for boundary lipid. *Biochemistry.* 18:3257–3267.
23. Lindblom, G., B. Lennart, A. Johansson, and G. Arvidson. 1981. Effect of cholesterol in membranes. Pulsed nuclear magnetic resonance measurements of lipid lateral diffusion. *Biochemistry.* 20:2204–2207.